TiO_2 Sol–Gel Nanomaterials: Synthesis, Properties and Applications

Dmitry Kovalenko, Vladimir Gaishun, Vasily Vaskevich, Alina Semchenko, and Olim Ruzimuradov

Abstract The present study examines the synthesis, properties, and applications of nanostructured materials based on titanium dioxides (TiO_2) via the sol–gel method. The sol–gel method makes it possible to vary the physicochemical properties of nanostructured materials over a wide range and achieve significant interaction between components at the stage of the initial sol. Simultaneously, sol–gel synthesis of nanostructured materials is more energy efficient compared to vacuum and plasma methods. The main physical and chemical processes that occur throughout the preparation and maturation stages of sol are determined. The influence of synthesis conditions on the dispersion, phase composition, and properties of nanostructured materials based on titanium dioxide is established. A description of the sol–gel method for producing bulk nanostructured materials is provided. Extensive studies have been conducted to examine the optical and structural properties of nanostructured materials based on TiO_2. Numerous investigations have been carried out on the photocatalytic activity of nanostructured films and xerogels obtained through the sol–gel method. The study findings indicate that nanostructured films and xerogels derived from TiO_2 possess photocatalytic properties, making them suitable for application in water purification systems.

Keywords TiO_2 · Sol–gel method · Nanostructured films · Optical properties · Photocatalytic activities

D. Kovalenko (✉) · V. Gaishun · V. Vaskevich · A. Semchenko
Francisk Skorina Gomel State University, Sovetskaya 104, 246028 Gomel, Belarus
e-mail: dkov@gsu.by

O. Ruzimuradov
National University of Uzbekistan Named After Mirzo Ulugbek, Student's Campus, University Street 4, Tashkent, Uzbekistan 100174

J. Prakash et al. (eds.), *Titanium Dioxide-Based Multifunctional Hybrid Nanomaterials*, Engineering Materials, https://doi.org/10.1007/978-3-031-80625-4_3

1 The Main Stages of Photocatalytic TiO_2 Sol–Gel Nanomaterials Synthesys

1.1 Stable Sols Based on Organic Titanium Compounds

The hydrolysis of various titanium compounds (alkoxides and inorganic titanium salts, mainly $TiCl_4$) in aqueous solutions leads to primary products at low pH values such as basic salts of variable composition. At higher pH values, hydrated forms of TiO_2 are formed, which correspond to the formula $Ti(OH)_2$ or titanium dioxide $(TiO_2)\cdot nH_2O$, where n depends on aging and drying conditions.

Freshly precipitated hydrated TiO_2 has a high adsorption capacity for both cations and anions; the content and nature of impurities in TiO_2 depend on the pH of the medium during precipitation, the nature of the precipitant, and the initial titanium compound.

The specific surface area of the hydrated TiO_2 generated during hydrolysis under hydrothermal conditions also significantly depends on the temperature and duration of the process. The available data indicates that the degree of crystallization of the product resulting from hydrothermal hydrolysis is greatly affected by the initial concentration of $TiCl_4$, which determines the acidity of the reaction environment.

The photocatalysis mechanisms by which certain types of organic compounds are decomposed completely to carbon dioxide and water are well known. New materials have been developed based on titania, and the sensitivity to visible light has improved [1]. The generation of new catalytic active sites either on the silica surface or in the silica matrix is discussed and the insights obtained from these studies allow a fundamental understanding of the relationships between the structural characteristics and the physico-chemical/reactivity properties of titania–silica catalysts [2]. Titania–silica materials represent a novel class of catalysts and have been widely applied in photocatalysis, acid catalysis and oxidation catalysis. The intimate interaction of TiO_2 and SiO_2 has been shown to result in new structural characteristics and physicochemical/reactivity properties. The degree of interaction, in other words, the homogeneity or dispersion when TiO_2 is mixed with or supported on SiO_2, largely depends on the preparation methods and synthesis conditions. Also, the surface enrichment of either Ti or Si in TiO_2–SiO_2 mixed oxides has been shown to depend on the preparation conditions and chemical compositions [2].

The possibilities for the purposeful control and stabilization of properties of TiO full control and stabilization of properties of TiO_2 nanopowders and sols are very wide [3]. Particles of titanium dioxide and titanium dioxide-hydroxypropyl cellulose organic–inorganic composite can be easily synthesized by the sol–gel method [4].

A simple and accessible method for obtaining pure and stable nanosized TiO_2 (anatase) under mild hydrothermal conditions is well known. Performing solvothermal hydrolysis of titanium ethoxide in anhydrous ethanol with the addition of a strictly defined amount of ultrapure water under mild conditions also results in the production of pure ultrafine dispersed nanocrystalline anatase [5, 6].

TiO_2 exists in the form of several crystalline modifications. Anatase, rutile, and brookite can be found in nature. Note that brookite is seldom manufactured on an industrial scale and is rarely encountered in nature. The anatase form is also significantly inferior in production volume to rutile, since rutile dioxide scatters light approximately 30% better (better hiding power) and is more weather-resistant. When heated, both anatase and brookite are irreversibly converted to rutile (transition temperatures, respectively, (400–1000) °C and about 750 °C).

During heat treatment of gels, hydrated forms of TiO_2, they crystallize with the formation of anhydrous TiO_2. Depending on the calcination temperature, polymorphic transformations of hydrated TiO_2 into anatase, rutile, or brookite are possible. These transformations are followed by changes in the specific surface area and porous structure. At temperatures below 600 °C, the crystallization process occurs with the formation of anatase with practically unchanged pore volume and specific surface area. At higher temperatures, a transition of anatase to rutile is observed, accompanied by a sharp decrease in both pore volume and specific surface area. The temperature of polymorphic transformation can also be greatly influenced by mineral impurities. Numerous data have shown that, in addition to the phase composition, the conditions of heat treatment of TiO_2 gels determine other important performance characteristics of TiO_2—morphology and particle size [7].

The most common methods for producing TiO_2 are sulfate and chloride (from $TiCl_4$). The processing of titanium tetrachloride is carried out according to three different schemes: hydrothermal hydrolysis, vapor-phase hydrolysis or combustion in a stream of oxygen. Recently, the sol–gel method, which is suitable for obtaining nanosized TiO_2 particles with a given structure and properties, has become increasingly important and, therefore, is of interest in connection with its application in the field of nanotechnology. Materials based on TiO_2 have extremely diverse applications: as photocatalytic, antibacterial, antireflective coatings [8–21]; coatings to protect the surface from various influences [18, 20–28]; coatings for solar cells [29–31].

The hydrolysis of various titanium compounds (alkoxides and inorganic titanium salts, mainly ethoxides) in aqueous and anhydrous solutions leads to primary products at low pH values such as basic salts of variable composition. This research employs titanium ethoxide as the initial alcohol compound to obtain film-forming solutions. This is because the hydrolysis of titanium ethoxide in anhydrous isopropyl alcohol with the addition of a strictly defined amount of ultrapure water under mild conditions leads to the formation of a stable solution.

1.2 Formation of Thin Films of Titanium Oxide.

The spin-coating procedure is the optimal technique for obtaining coatings on flat substrates.

The centrifugal application method involves the formation of a deposited layer by spreading the film-forming solution under centrifugal forces. The excess film-forming solution is forced out of the substrate in a radial flow due to the effect of centrifugal force.

It is well-known that the main parameters influencing the thickness of sol–gel coatings produced via centrifugation are the viscosity of the film-forming solution and the rotation frequency of the substrate. Experiments were conducted to determine the optimal range of rotation speeds for the workpieces in relation to the selected sol. These experiments involved the deposition of sol–gel films on substrates of various sizes by centrifugation. A series of experiments established a correlation between the diameter of the substrate and the rotation frequency at which the resulting films have a minimum width of the brim formed by the coating at the edge of the substrate surface.

Ready-made film-forming solutions were deposited on previously prepared substrates made of silicon, quartz glass, and metal using centrifugation and dipping methods. After deposition, the resulting samples were heat-treated step by step in air from 100 to 800 °C.

1.3 Formation of Bulk Materials Based on TiO_2

The method for obtaining bulk photocatalytic materials includes the following stages:

1. Obtaining a sol by hydrolysis in a water solution in the presence of nitric acid as a catalyst. The hydrolysis of titanium-based sols was carried out in an anhydrous environment. The starting components were mixed in a special polymer reactor with a paddle stirrer for 30 min;
2. Fine dispersion under ultrasonic conditions;
3. Centrifugal separation of solid particles and impurities at a centrifuge rotation speed of 3000 rpm for 60 min;
4. For neutralizing the acidic environment and accelerating the gelation process, drops of a 0.1 N alkali solution are added to the mixture to increase the pH to 4–6. Casting the sol into molds and gelling for 15–30 min at room temperature;
5. Maturation of gels during the day;
6. Formation of xerogels by drying the gels in an oven at a temperature of 40–50 °C for 3–5 days, depending on the geometric dimensions of the gels.

Figure 1 presents a schematic diagram illustrating the process of creating xerogels doped with noble metals and rare earth elements.

The hydrolysis rate is influenced by many factors, in particular the presence of a catalyst, temperature, solvent concentration, etc.

Controlling the structure of TiO_2 at the nanoscale can lead to significant improvements in the functional properties of the resulting material. By employing the sol–gel technique, it becomes feasible to not only regulate and reproduce the ratio of TiO_2

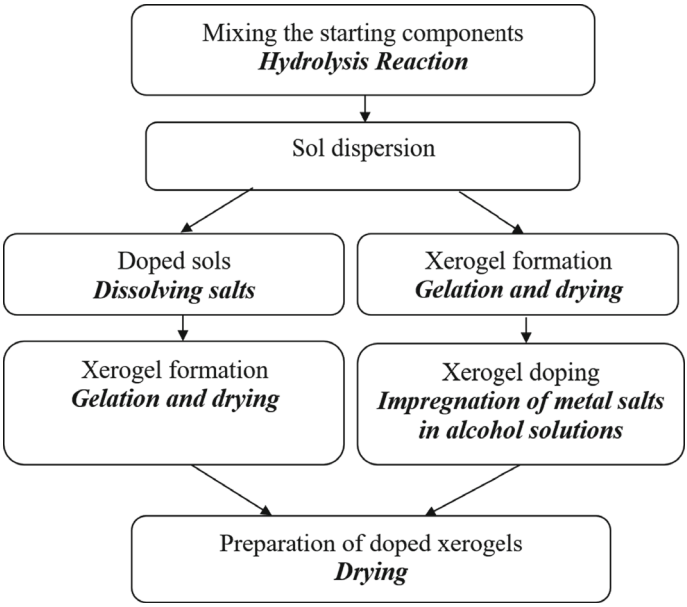

Fig. 1 Schematic diagram illustrating the formation of xerogels doped with metals

crystalline phases (anatase, rutile, and brookite) in the resulting product, but also to obtain each phase in its pure form [5, 6].

Preparing the sols to obtain gels and xerogels from titanium isopropoxide and titanium ethoxide as detailed below. The synthesis was carried out in a glass vessel. Previously, a hydrolysis mixture was placed in the flask, which consisted of isopropyl alcohol and concentrated hydrochloric or nitric acid. Titanium isopropoxide or titanium ethoxide was added to the flask while stirring continuously. The resulting mixture was homogenized. The hydrolysis of titanium alkoxides can be represented by the following equations:

$$\mathrm{Ti-OR + H_2O \rightarrow Ti-OH + ROH},$$
$$\mathrm{Ti-OH + Ti-OR \rightarrow Ti-O-Ti + ROH},$$
$$\mathrm{Ti-OH + Ti-OH \rightarrow Ti-O-Ti + HOH}.$$

Sols of various compositions containing titanium isopropoxide or titanium ethoxide were prepared since the resulting structure, which determines the structural characteristics, strongly depends on the preparation conditions, including the composition of the initial components.

1.3.1 Formation of Doped Xerogels by Gelation

Gelation in alkoxide sol–gel processes occurs spontaneously and continues for several days. Nevertheless, with a rise in temperature, the gelation time experiences a substantial decrease.

To create homogeneous matrices with optimal parameters (formation of solid gel blanks, obtaining a given xerogel porosity, etc.), the type and amount of the introduced solid filler, TiO_2 powder, play a decisive role. It was found that introducing a filler, for example, directly into the hydrolyzate product leads to its clumping and, consequently, to the presence of large agglomerates of particles in the final ash. Therefore, the dispersion of the filler in an aqueous environment is separated into a distinct process [7].

Depending on the calcination temperature, polymorphic modifications of hydrated TiO_2 into anatase, rutile or brookite are possible, accompanied by changes in the specific surface area and porous structure. The sol–gel method allows for regulation and reproduction of the crystalline phase ratio of TiO_2 (anatase, rutile, and brookite) in the resulting product while also obtaining each phase in its pure form [8–21].

1.3.2 Formation of Xerogels by Pressing

After obtaining a xerogel for photocatalytic purification based on TiO_2, a porous structure (tablets with a diameter of 1.6 cm and a thickness of 1 cm) was created by compression molding in order to enhance the working surface, which will interact with the solution during the photocatalysis process. The resulting xerogels, after mixing with TiO_2 powder, were placed in a mold to form tablets. Initial solutions based on titanium compounds were used as a binder and a plasticizer when forming the workpieces.

Subsequently, the resulting tablets were subjected to a step-by-step heat treatment process in order to produce the photocatalytically active polymorphic modification rutile or brookite.

The materials were placed in an oven and heat-treated at 600 and 800 °C for 60 min, followed by cooling in air.

The materials obtained via this method can be used as targets to form coatings from the plasma of a pulsed cathode-arc discharge. In order to accomplish this, the dried xerogels are annealed at a temperature of 900–950 °C for 6 h, which causes the formation of a ceramic material. During annealing, numerous complex physical and chemical processes occur which are related to the degradation of organic fragments embedded in the inorganic gel network, the removal of solvents, volatile degradation products, and chemically bound water. The inorganic polymer undergoes a restructuring process known as sintering, which may also involve crystallization in certain instances.

2 Properties of TiO_2 Sol–Gel Nanomaterials

2.1 Calculation of the Refractive Index of the Resulting Thin Films

The refractive index of a TiO_2 coating can be determined by using the absorption maximum observed in the transmission spectrum. For a weak absorptive coating, assuming normal light incidence, the minimum transmittance is calculated as follows:

$$T_{\min} = 4n_f^2 n_s / \left(n_f^2 + n_s^2\right).$$

The coating refractive index

$$n_f = \left[n_s(2 - T_{\min}) + 2n_s(1 - T_{\min})^{1/2}/T_{\min}\right]^{1/2},$$

where n_f is the refractive index of the coating, n_s is the refractive index of the substrate [32].

Table 1 shows that as the heat treatment temperature is raised, the refractive index of the coating exhibits a gradual increase. This phenomenon is explained by the fact that with the refractive index of the anatase structure of 2.23, rutile is denser, i.e., its refractive index is 2.60. The coating samples after heat treatment at 700 °C represent an anatase structure. At 800 °C, the samples represent a mixed structure of anatase and rutile. When temperature reaches 900 °C, the coating structure changes to the rutile phase, showing the maximum refractive index. Achieving precise tuning of the optical properties of the TiO_2 coating requires careful control of the ratio between the two structural structural types, anatase and rutile. This ratio is susceptible to alteration during heat treatment, thereby causing a modification in the refractive index.

Table 2 illustrates that increase in the annealing temperature is accompanied by the gradual increase in the refractive index of the coating. This phenomenon is explained by the fact that when the refractive index of the mixed structure of anatase and rutile is 2.10, rutile is denser, i.e., its refractive index is 2.55. Following heat treatment at 500 °C, the coating samples represent a mixed structure of anatase and rutile; after heat treatment at 900 °C, the structure completely transforms into the rutile phase, showing the maximum refractive index.

Table 1 Refractive index of TiO_2 (isopropoxide) coatings

Annealing temperature	600 °C	700 °C	800 °C	900 °C
Refractive index	2.17	2.23	2.55	2.60

Table 2 Refractive index of the TiO_2 coatings

Annealing temperature	500 °C	600 °C	800 °C	900 °C
Refractive index	2.10	2.20	2.36	2.55

2.2 *Structural Properties of Synthesized Sol–Gel Coatings Using Raman Spectroscopy*

The Raman spectrum was recorded using a SENETRA express Raman spectrometer (Bruker).

The analysis revealed that the TiO_2 coating captures oxygen from the atmosphere during the annealing process. Additionally, the annealing temperature promotes surface modification, grain growth, grain bonding, and the growth and development of the crystalline structure (Figs. 2 and 3).

Annealing at a temperature of 600 °C leads to the emergence of Raman peaks at 639, 513, 392 and 148 cm^{-1}. These vibrations correspond to the structure of the TiO_2 coating, i.e., anatase. The transition from the amorphous structure to the crystalline phase of anatase begins at an annealing temperature of 600 °C.

Increasing the annealing temperature up to 700 °C leads to a gradual increase in the intensity of the lines in the TiO_2 spectrum and a corresponding rise in the degree of crystallization of the coating. However, it is important to note that the rutile phase does not occur at these temperatures. The peaks of the coating, which includes titanium ethoxide, at frequencies of 148, 392, 513 and 639 cm^{-1} are much more intense than the peaks of the coating, which includes titanium isopropoxide. It can be seen that

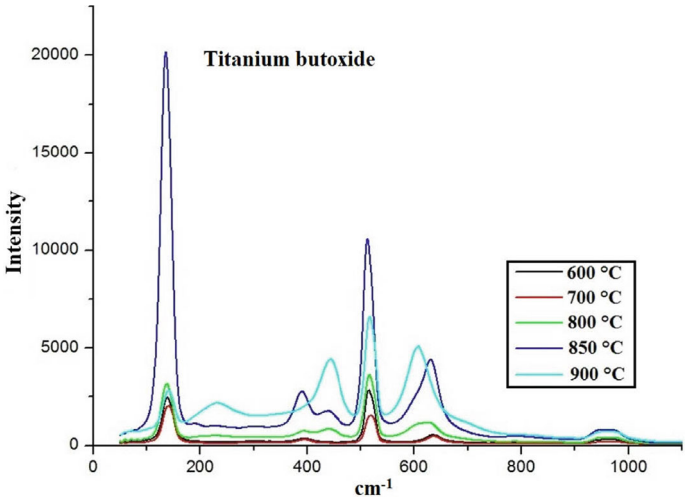

Fig. 2 Raman spectrum of TiO_2 coatings at different annealing temperatures

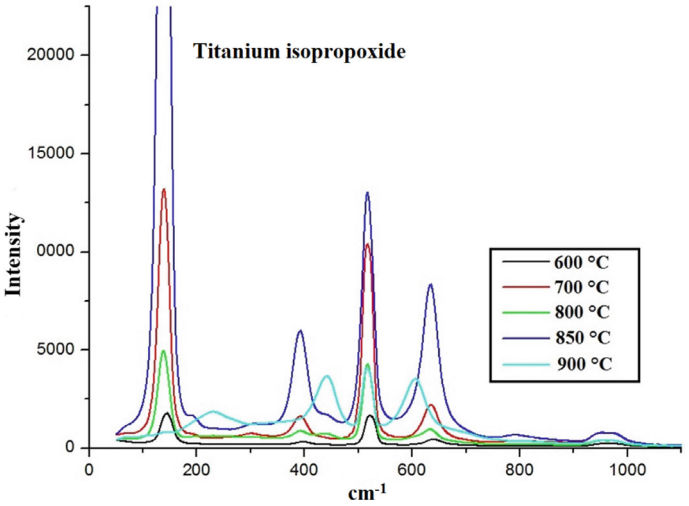

Fig. 3 Raman spectrum of TiO_2 coatings based on titanium isopropoxide at different annealing temperatures

at annealing temperatures of 600~700 °C, the TiO_2 coating predominantly exhibits a crystalline structure within the anatase phase.

The intensity of the coating peaks characterizing the anatase phase experienced a substantial increase after annealing at a temperature of 800 °C. The coating, including ethoxide, exhibits a novel distinctive peak at a frequency of 441 cm^{-1}, which corresponds to the structure of rutile TiO_2. The intensity of the peak is weak. This spectrum indicates that the structure of the TiO_2 coating is in the early stages of transitioning from the anatase phase to the rutile phase.

At 850 °C, the peaks of the coating, which contained isopropoxide, representing the anatase phase at frequencies of 398 and 640 cm^{-1}, nearly vanished. The intensity of anatase peaks at frequencies of 513, 148, 392 and 639 cm^{-1} is significantly reduced. Intensity peaks appeared at 441 and 607 cm^{-1}, which characterize the rutile phase.

At an annealing temperature of 900 °C, the intensity of the peaks in the Raman spectrum of the coating at frequencies of 607 cm^{-1} and 441 cm^{-1} exhibited a substantial increase, whereas the peaks at frequencies of 392 cm^{-1} and 639 cm^{-1} disappeared. Furthermore, in the case of the coating containing isopropoxide, the peak at 148 cm^{-1} vanished. The peak at 513 cm^{-1} decreased significantly. A new intensity peak appeared at a frequency of 235 cm^{-1}, which characterizes the rutile structure. The TiO_2 coating almost completely crystallizes into the rutile phase.

The above-described analysis demonstrates that as the annealing temperature is raised, the structure of the TiO_2 coating transforms from amorphous to rutile. The rutile phase exhibits superior thermal stability in comparison to the anatase phase. This property is shared by anatase and rutile, despite the fact that they both represent a tetragonal system. The rutile phase represents an octahedron with a shared face

and vertex, while the anatase phase is an octahedron with a shared vertex. Such a structure is unstable. Therefore, from a thermodynamic point of view, the rutile phase is a stable structure at high temperatures of TiO_2. In addition, due to the fact that the density of the amorphous coating (3.2~3.65 g cm^{-3}) compared to the density of rutile (4.26 g cm^{-3}) is much lower, the structure of the coating is converted from an amorphous state to rutile. This is accompanied by a process of significant compaction of the substance, while the binding energy is greater than during the formation of anatase (3.2 g cm^{-3}). Similarly, when the annealing temperature increases, the phase transition of TiO_2 proceeds as follows: amorphous–anatase–rutile.

2.3 Structural Properties via X-ray Phase Analysis

The study of structural properties by X-ray phase analysis was carried out on samples of titanium oxide that underwent heat treatment from 400 to 800 °C. Previously, when analyzing Raman spectra, it was found that at annealing temperatures above 800 °C, the content of the anatase phase in the sample decreases, due to which the materials have pronounced photocatalytic properties.

The results of X-ray phase analysis indicate that low-temperature annealing ($T \leq 400$ °C) does not lead to the formation of active TiO_2 particles in the resulting films. The diffraction patterns of films, fabricated on the basis of titanium ethoxide (Fig. 4), show that TiO_2 crystals transforming into the brookite phase and subsequently functioning as active centers in photocatalytic reactions are formed at temperatures $T \geq 600$ °C.

With a further increase in the heat treatment temperature to 800 °C, there is an increase in the intensity of the lines due to the presence of brookite in the coatings ($2\theta = 25.24°$). This modification of TiO_2 is superior in photocatalytic activity to anatase and rutile [4]. The intensity of the Ti_2O_3 peaks ($2\theta = 61.55°$) decreases with increasing the annealing temperature from 600 to 800 °C. Thus, the presence of brookite in the thin-film systems under study makes it possible to use them as coatings with a self-cleaning surface, as well as to create water purification systems based on filters made from a set of metal meshes with an active photocatalytic coating [7].

2.4 Surface Properties of the Resulting Sol–Gel Coatings via AFM Spectroscopy

Figure 5 shows the morphology of TiO_2 (isopropoxide) coatings obtained through the sol–gel method after annealing at different temperatures. It is evident from the figure that during annealing at 400 °C, the surface is composed of particles that have an irregular shape and blurred boundaries. This may be due to the low annealing

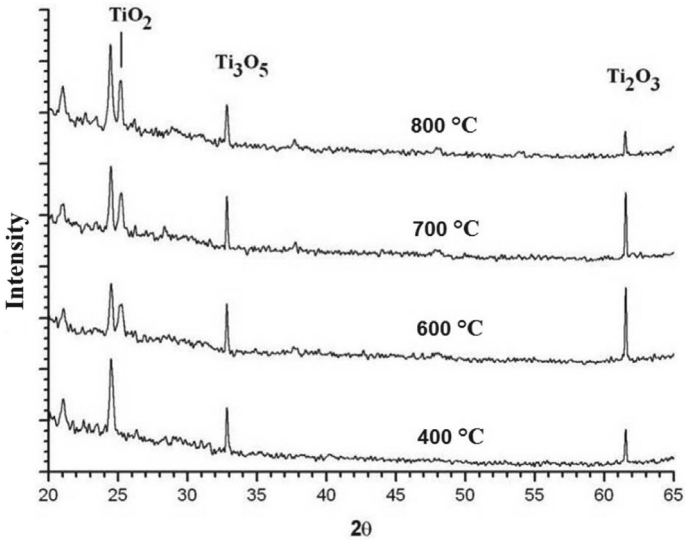

Fig. 4 Diffraction patterns of sol–gel coatings, formed on the basis of titanium ethoxide

temperature. The degree of crystallization is low, resulting in the blurred boundary between grains and a decrease in the grain size.

Following the annealing process at 600 °C, it is obvious that the particles present on the coating's surface exhibit an even distribution, a considerable degree of crystallinity, and distinct boundaries between grains.

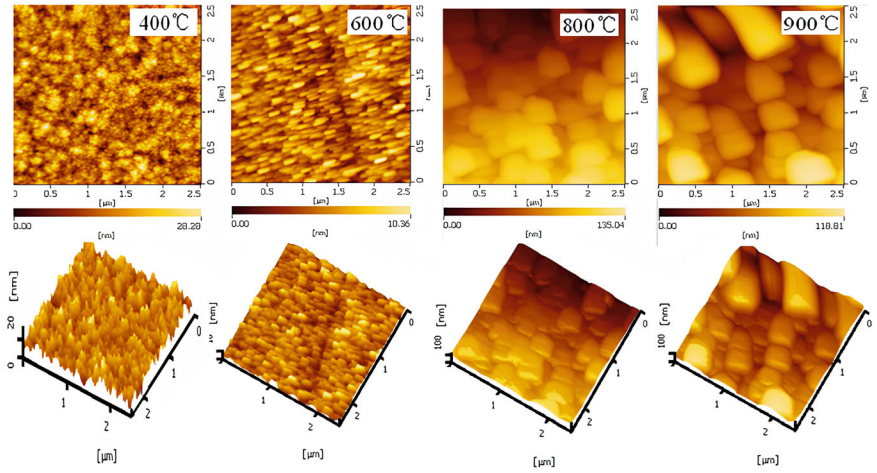

Fig. 5 AFM images of TiO_2 coatings based on titanium isopropoxide obtained at different annealing temperatures

Table 3 Surface roughness parameters

Annealing temperature	400 °C	600 °C	800 °C	900 °C
Relief microroughness R_z, nm	385.1	421.3	61.5	56.9
Mean absolute error from profile points to the center line R_a, nm	5.8	9.3	2.6	4.4
Roof-mean-square deviation from profile points to the center line R_q, nm	18.2	24	4.5	6.4

Upon annealing at 800 °C, the grain size of the coating surface grew larger, the particles became densely packed, and the grain morphology was accurate. The surface structure changed significantly compared to the structure of the coating when subjected to annealing at a temperature of 600 °C. The structural analysis of the TiO_2 coating shows that the coating contains two phases, anatase and rutile.

An elevation in the annealing temperature generates sufficient energy to facilitate complete crystallization within the rutile phase, thereby promoting an increase in the grain size. After annealing at 900 °C, the grain size reached 200 nm in the TiO_2 coating.

According to the data presented in Table 3, the relief microroughness (R_z) is equal to 385.1 nm when annealed at 400 °C. It implies that the surface is composed of irregularly shaped particles. This may be due to the low annealing temperature. The degree of crystallization is low, which blurs the boundary between grains and reduces the grain size.

Upon annealing at 600 °C, the relief microroughness R_z exhibited an increase to 421.3 nm. This phenomenon can be attributed to the formation of the anatase phase, which takes place at this specific annealing temperature. This is evident from the structural analysis of the TiO_2 coating.

After subjecting the coatings to annealing at 800 °C, there was a notable alteration in the surface structure, in contrast to the structure observed at the annealing temperature of 600 °C. The relief microroughness decreased to 61.5 nm. When temperature reached 900 °C, the R_z index reduced to 56.9 nm. which indicates that the coating structure underwent a transition to the rutile phase.

2.5 Photocatalytic Properties of TiO_2 Sol–Gel Materials

Heterogeneous photocatalysis using titanium dioxide-based materials is considered a promising and innovative solution to the water pollution problem. The challenge is to convert the basic research into a successful innovation, leading to the implementation of this process into wastewater treatment [13, 14]. Currently, TiO_2-based photocatalytic membranes are at the forefront of photodegradation research and technical readiness. The membrane setup provides a high contact surface area for effective filtration and degradation, without the necessary hassle of photocatalyst recovery

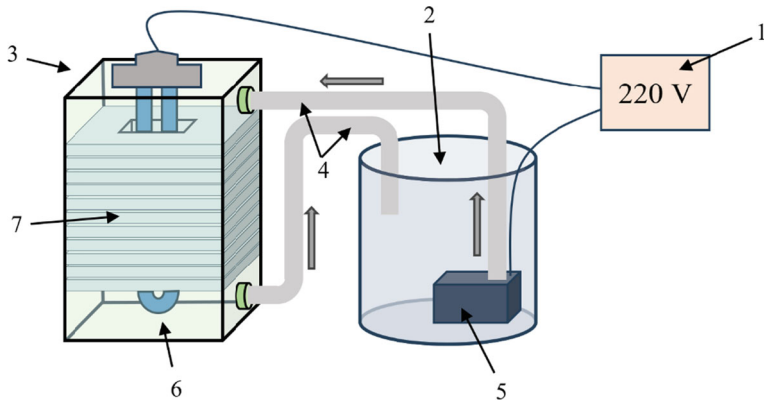

1 – power supply; 2 – flask; 3 – chamber;
4 – rubber hoses; 5 – pump; 6 – UV lamp;
7 – filter made of a series of brass meshes with a photocatalytic coating

Fig. 6 Diagram illustrating the setup for studying the photocatalytic properties of the resulting coatings

after water and wastewater treatment [15, 16]. The other way is the using of TiO_2 and Ag/TiO_2 nanoparticles to influence on the oxidation of organic matter of domestic wastewater was evaluated using a heterogeneous photocatalytic system [17, 18].

The photocatalytic activity of the materials was studied using model reactions of photocatalytic oxidation of methylene blue ($C_{16}H_{18}ClN_3S{:}H_2O$) in an aqueous solution subjected to ultraviolet irradiation. The dye concentration was $5{\cdot}10^{-3}$ wt.%. This was sufficient for the initial solution to possess a rich blue color. Xerogels were placed in the chamber of the setup, and the chamber was then filled with a solution of methylene blue.

For these purposes, an experimental setup was constructed, consisting of a chamber with an ultraviolet light emitter and a brass mesh filter with a photocatalytic coating (Fig. 6).

The volume of the chamber was designed considering the dimensions of the UV radiation source and the maximum capacity of the setup. The chamber parts were assembled using screw connections. A small-sized fluorescent U-shaped lamp was used as a radiation source, emitting in the ultraviolet and visible range of the radiation spectrum from 300 to 450 nm. The solution was supplied to the working chamber of the installation using SOBO Internal Filter WP–330F.

In order to investigate the photocatalytic properties of bulk materials, ceramic blanks that had been manufactured in advance were substituted for plates and the experiment was re-conducted.

The photocatalytic properties of the films and bulk xerogels were assessed by the decomposition of an organic dye, methylene blue ($C_{16}H_{18}ClN_3S{:}H_2O$), in an aqueous solution subjected to ultraviolet radiation. The dye concentration was $5{\cdot}10^{-3}$ wt.%. This was sufficient for the initial solution to have a rich blue color.

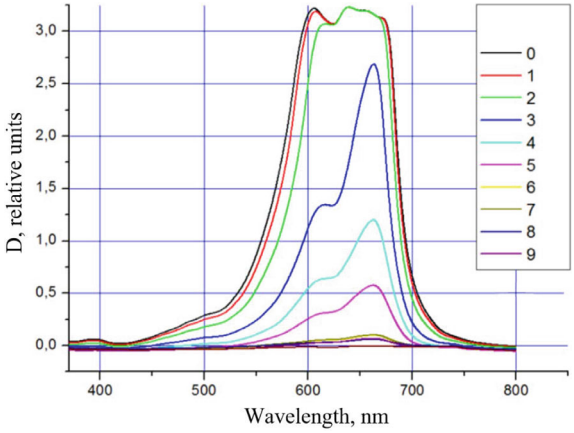

Fig. 7 Absorption spectra of the methylene blue solution for a filter made from a series of meshes deposited with photocatalytic films

Brass meshes were used to study the photocatalytic properties of the films. The film samples were deposited by dipping. Then the meshes were placed in the chamber. The irradiation time was 9 h. Water sampling were performed every 60 min. Additionally, a sample was taken that contained a dye solution that had not been exposed to radiation. The decomposition of the dye was monitored by changes in its optical transmission spectra in the visible wavelength range.

The photocatalytic properties of the resulting coatings were controlled by observing changes in the optical absorption spectra of a methylene blue solution within the visible wavelength range. The absorption spectra are presented in Fig. 7.

The photocatalytic properties of bulk xerogels were studied in a similar way. The xerogels were placed in the chamber of the setup, and the chamber was filled with a solution of methylene blue.

The absorption spectra of the methylene blue solution for a filter made of bulk xerogels are provided in Fig. 8.

Analyzing the collected absorption spectra, it becomes evident that the intensity of the absorption peak decreases over time. Within nine hours, the absorption peak, which was localized at a wavelength of $\lambda = 659$ nm, reduced from 3.5 to 0.2 rel. units for films and bulk xerogels, which is a consequence of methylene blue photocatalytic oxidation. Consequently, the concentration of methylene blue in the solution also decreases due to its decomposition in the solution.

According to the results, it can be claimed that samples of coatings and xerogels containing TiO_2 exhibit photocatalytic activity and can be employed for the purpose of water purification.

After analyzing the findings of investigations concerning the photocatalytic properties of the resulting materials (Figs. 9 and 10), it can be concluded that samples subjected to heat treatment at 700 and 800 °C exhibit less pronounced photocatalytic abilities in contrast to samples subjected to heat treatment at temperatures ranging from 400 to 600 °C. The outcome is predominantly influenced by the anatase phase

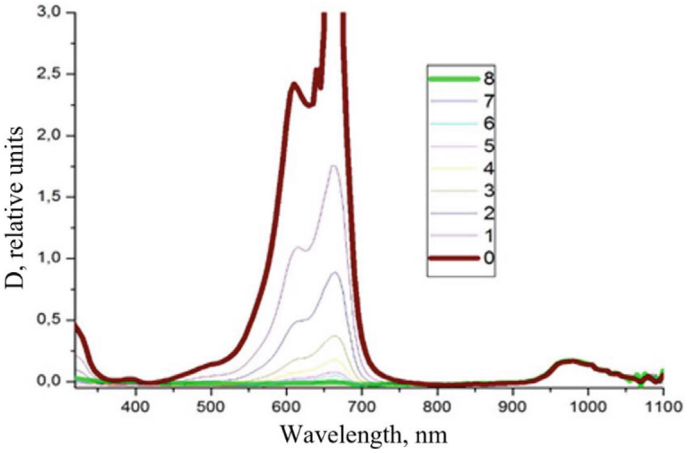

Fig. 8 Absorption spectrum of solution samples

concentration in titanium oxide, which imparts more prominent photocatalytic properties. Additionally, elevated temperatures (approximately 700 °C) result in a greater rutile phase content, which diminishes the photocatalytic properties.

The study's findings revealed a decrease in the methylene blue concentration in the solution to 1–2% of its initial concentration, which provides further evidence for the photocatalytic activity of coatings and xerogels based on TiO_2.

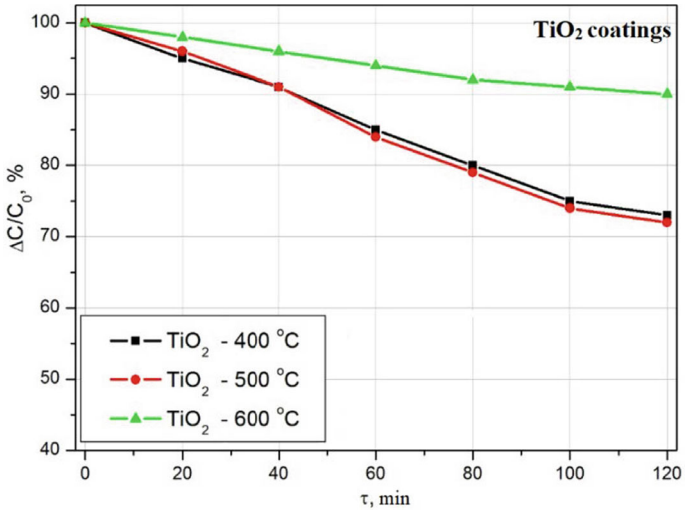

Fig. 9 Change in dye concentration—methylene blue during photocatalytic degradation on samples of TiO_2 coatings

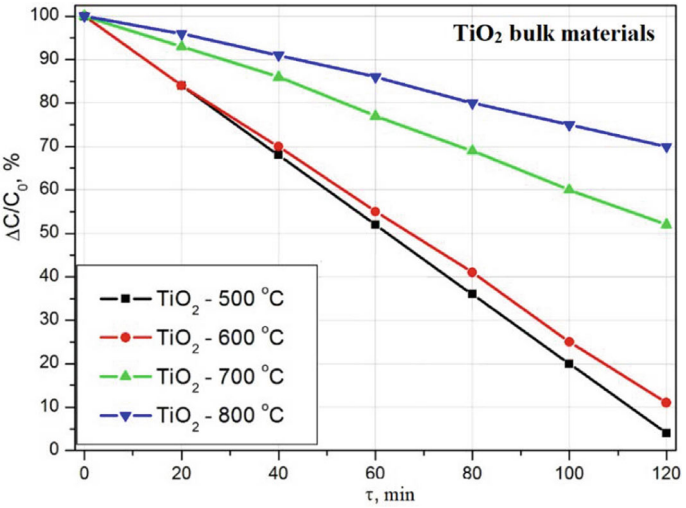

Fig. 10 Change in dye concentration—methylene blue during photocatalytic degradation on samples of TiO_2 bulk materials

3 Conclusion

An examination of the structural properties of the TiO_2 films generated at temperatures exceeding 600 °C through X-ray phase analysis revealed the presence of brookite-shaped TiO_2 crystals, which functioned as active centers in photocatalytic reactions. The influence of the concentration of cerium ions on the surface morphology of the resulting coatings was studied via the AFM method. It has been established that titanium films doped with cerium are characterized by the presence of pores, the size and number of which depend on the concentration of cerium salt in the original film-forming ash. The research results on the photocatalytic properties of cerium-doped TiO_2 films, using the example of the photocatalytic oxidation of methylene blue, show a decrease in the concentration of methylene blue in solution to 1–2% of its initial concentration. Coatings that have been developed can find their application as oxidative photocatalytic materials in small-scale cyclic water purification systems.

References

1. Fujishima, A., Zhang, X., Tryk, D.A.: TiO photocatalysis and related surface phenomena. Surf. Sci. Rep. **63**, 515–582 (2008). https://doi.org/10.1016/j.surfrep.2008.10.001
2. Xingtao, G., Wachs, I.E.: Titania-silica as catalysts: molecular structure characteristics and physico-chemical properties. Catal. Today. **51**, 233–254 (1999). https://doi.org/10.1016/S0920-5861(99)00048-6

3. Ismagilov, Z.R.: Synthesis and stability of nanosized titanium dioxide. Adv. Chem. **9**, 942–953 (2009). https://doi.org/10.1070/RC2009v078n09ABEH004082
4. Kraev, A.S., Agafonov, A.V., Davydova, O.I., et al.: Sol-gel synthesis of titanium dioxide and titanium dioxide-hydroxypropyl cellulose hybrid material and electrorheological characteristics of their dispersions in poly(dimethylsiloxane). Colloid J. **69**, 620–626 (2007). https://doi.org/10.1134/S1061933X07050122
5. Jia, Z.M., Zhao, Y.R., Shi, J.N.: Adsorption kinetics of the photocatalytic reaction of nano-TiO_2 cement-based materials: a review. Constr. Build. Mater. **370**, 130462 (2023). https://doi.org/10.1016/j.conbuildmat.2023.130462
6. Zhu, Z., Lu, Y., Zhou, M.: Surface modification of recycled tire rubber powders with Tannic acid and Nano-TiO_2 for enhanced performance and photocatalytic properties of Rubberized Cement-Based materials. Constr. Build. Mater. **399**, 132607 (2023). https://doi.org/10.1016/j.conbuildmat.2023.132607
7. Kovalenko, D.L., Gaishun, V.E., Vaskevich, V.V., Khakhomov, S.A., Khudaverdyan, S.K., Ayvazyan, G.Y.: Formation and research of properties of photocatalytic materials on the basis of TiO_2 for water treatment. In: Várkonyi-Kóczy, A. (eds.) Engineering for Sustainable Future. INTER-ACADEMIA 2019. Lecture Notes in Networks and Systems, vol. 101. Springer, Cham (2020). https://doi.org/10.1007/978-3-030-36841-8_4
8. Madkhali, N. et al.: Recent update on photocatalytic degradation of pollutants in waste water using TiO_2-based heterostructured materials. Results Eng. **17**, 100920 (2023). https://doi.org/10.1016/j.rineng.2023.100920
9. Wei, P., Zhang, Y., Huang, Y., Chen, L.: Structural design of SiO_2/TiO_2 materials and their adsorption-photocatalytic activities and mechanism of treating cyanide wastewater. J. Mol. Liq. **377**, 121519 (2023). https://doi.org/10.1016/j.molliq.2023.121519
10. McCormick, W.J., McCrudden, D., Skillen, N., Robertson, P.K.J.: Electrochemical monitoring of the photocatalytic degradation of the insecticide emamectin benzoate using TiO_2 and ZnO materials. Appl. Catal. A: Gen. **660**, 119201 (2023). https://doi.org/10.1016/j.apcata.2023.119201
11. Shi, Y., Zhang, Z., Dai, Y. et al.: Influence of current density on the photocatalytic activity of Nd:TiO_2 coatings. J. Wuhan Univ. Technol.-Mat. Sci. Edit. **39**, 32–38 (2024). https://doi.org/10.1007/s11595-024-2851-4
12. Jia, L., Yang, L.M., Wang, W., et al.: Preparation and characterization of Rb-doped TiO_2 powders for photocatalytic applications. Rare Met. **43**, 555–561 (2024). https://doi.org/10.1007/s12598-019-01241-2
13. Musial, J., Mlynarczyk, D.T., Stanisz, B.J.: Photocatalytic degradation of sulfamethoxazole using TiO_2-based materials—perspectives for the development of a sustainable water treatment technology. Sci. Total Environ. **856**(2), 159122 (2023). https://doi.org/10.1016/j.scitotenv.2022.159122
14. Yu, Y., Wana, J., Parr, J.F.: Preparation and properties of TiO_2/fumed silica composite photocatalytic materials. Procedia Eng. **27**, 448–456 (2012). https://doi.org/10.1016/j.proeng.2011.12.473
15. Wang, Q., et al.: Axial suspension plasma sprayed Ag-TiO_2 coating for enhanced photocatalytic and antimicrobial properties. Surf. Interfaces. **45**, 103856 (2024). https://doi.org/10.1016/j.surfin.2024.103856
16. Kirk, C.H., et al.: TiO_2 photocatalytic ceramic membranes for water and wastewater treatment: technical readiness and pathway ahead. J. Mater. Sci. Technol. **183**, 152–164 (2024). https://doi.org/10.1016/j.jmst.2023.09.055
17. Estrada-Vázquez, R., Vaca-Mier, M., Bustos-Terrones, V., et al.: Assessment of TiO_2 and Ag/TiO_2 photocatalysts for domestic wastewater treatment: synthesis, characterization, and degradation kinetics analysis. Reac Kinet Mech Cat (2023). https://doi.org/10.1007/s11144-023-02557-y
18. Dontsova, T., Kyrii, S., Yanushevska, O., et al.: Physicochemical properties of TIO_2, ZrO_2, Fe_3O_4 nanocrystalline adsorbents and photocatalysts. Chem. Pap. **76**, 7667–7683 (2022). https://doi.org/10.1007/s11696-022-02433-4

19. Shilova, O.A., Glebova, I.B., Voshchikov, V.I., Ugolkov, V.L., Dolmatov, V.Yu., Komarova, K.A., Ivanova, A.G.: Environmentally friendly antifouling transparent coatings based on sol-gel "epoxy/titanium tetrabutoxide" composition modified with detonation nanodiamond. J. Adv. Mater. Technol. **7**(3), 201–218 (2022). https://doi.org/10.17277/jamt.2022.03
20. Kovalenko, D.L., Gaishun, V.E., Vaskevich, V.V., Aleshkevich, N.A.: Formation of sol-gel by the method of antireflective two-layer TiO_2-SiO_2 coatings. Vesti, Gomel State University named after F. Skorina, Gomel. **72**(3), 63–68 (2012)
21. Shilova, O.A., Vlasov, D.Y., Zelenskaya, M.S., Ryabusheva, Y.V., Khamova, T.V., Glebova, I.B., Sinelnikov, A.A., Marugin, A.M., Frank-Kamenetskaya, O.V.: Sol-gel derived TiO_2 and epoxy-titanate protective coatings: Structure, property, fungicidal activity and biomineralization effects. In: Frank-Kamenetskaya, O.V., Vlasov, D.Yu., Panova, E.G., Lessovaia, S.N. (eds.) Processes and Phenomena on the Boundary between Biogenic and Abiogenic Nature, pp. 619–638. Swizerland, Springer. (Scopus) (2020). ISBN 978-3-030-21613-9. https://doi.org/10.1007/978-3-030-21614-6_33
22. Shapovalov, V.I., Shilova, O.A., Smirnova, I.V., Zav'yalov, A.V., Lapshin, A.E., Magdysyuk, O.V., Panov, M.F., Plotnikov, V.V., Shutova, N.S.: Modification of the glass surface by titanium dioxide films synthesized through the sol–gel method. Glass. Phys. Chem. **37**, 150–156 (2011). https://doi.org/10.1134/S1087659611020143
23. Bouyarmane, H., et al.: Photocatalytic degradation of emerging antibiotic pollutants in waters by TiO_2/Hydroxyapatite nanocomposite materials. Surf. Interfaces. **24**, 101155 (2021). https://doi.org/10.1016/j.surfin.2021.101155
24. Bayan, E.M., Pustovaya, L.E., Volkova, M.G.: Recent advances in TiO_2-based materials for photocatalytic degradation of antibiotics in aqueous systems. Environ. Technol. Innovation. **24**, 101822 (2021). https://doi.org/10.1016/j.eti.2021.101822
25. Michael, M.P., Singh, S.K., Sahini, M.G.: Facile conglomeration of guar gum/TiO_2/Fe_3O_4 composite materials for photocatalytic antimicrobial activities. J. Indian Chem. Soc. **99**(10), 100688 (2022). https://doi.org/10.1016/j.jics.2022.100688
26. Pandele-Cusu, J., Petrescu, S., Preda, S., et al.: Comparative study of the TiO_2 nanopowders prepared from different precursors and chemical methods for heterogeneous photocatalysis application. J. Therm. Anal. Calorim. **147**, 13111–13124 (2022). https://doi.org/10.1007/s10973-022-11544-9
27. Dobromir, M., Konrad-Soare, C.T., Stoian, G., Semchenko, A., Kovalenko, D., Luca, D.: Surface wettability of ZnO-loaded TiO_2 nanotube array layers. Nanomaterials **2020**, 10 (1901). https://doi.org/10.3390/nano10101901
28. Lukong, V.T., Ukoba, K., Jen, TC.: Review of self-cleaning TiO_2 thin films deposited with spin coating. Int. J. Adv. Manuf. Technol. **122**, 3525–3546 (2022). https://doi.org/10.1007/s00170-022-10043-3
29. Ayvazyan, G.Y., Kovalenko, D.L., Matevosyan, L.A., Semchenko, A.V.: Investigation of the structural and optical properties of silicon-perovskite structures with a black silicon layer. J. Contemp. Phys.**57**(3), 274–279. https://doi.org/10.1134/S1068337222030069
30. Kovalenko, D.L., et al.: Development of a combined method for the formation of ZnO/TiO_2 nanotubes. Prob. Phys. Math. Tech. **49**(4), 11–16 (2021). https://doi.org/10.54341/20778708_2021_4_49_11
31. Semchenko, A.V., et al.: Characteristics of nanocomposite sol-gel films on black silicon surface. In: Khakhomov, S., Semchenko, I., Demidenko, O., Kovalenko, D. (eds.) Research and Education: Traditions and Innovations. INTER-ACADEMIA 2021. Lecture Notes in Networks and Systems, vol. 422. Springer, Singapore (2022). https://doi.org/10.1007/978-981-19-0379-3_21
32. Sanchez-Gonzalez, J., Diaz-Parralejo, A., Ortiz, A.L., Guiberteau, F.: Determination of optical properties in nanostructured thin films using the Swanepoel method. Appl. Surf. Sci. **252**, 6013–6017 (2006). https://doi.org/10.1016/j.apsusc.2005.11.009